engineering proceedings

MDPI

Proceeding Paper

Microstructure Evolution in a 6082 Alloy under Pulsed Magnetic Field Melt Treatment †

Xinyu Bao [1,2,*], Yonglin Ma [1,*] and Yongzhen Liu [1]

[1] School of Material and Metallurgy, Inner Mongolia University of Science and Technology, Baotou 014010, China; liuyz0424@163.com
[2] Beijing Yeke Electromagnetic Energy New Technology Co., Ltd., Beijing 100000, China
* Correspondence: bxyxinyu@163.com (X.B.); malin@imust.edu.cn (Y.M.)
† Presented at the 15th International Aluminium Conference, Québec, QC, Canada, 11–13 October 2023.

Abstract: The 6082 alloy is used to produce DC (direct-chilling) billets for subsequent forging or rolling processes. It is necessary to control the solidification structure in casting billets during the casting process. Based on the previous work, the energy of the magnetic field was found to reduce the formation work of the larger cluster in the melt, leading to the formation of larger clusters in the melt, facilitating nucleation and refining the solidification structure. Inspired by this, the pulsed magnetic field melt treatment was applied upon the launder of the casting platform to affect the morphology, size and distribution of α-Al dendrites in the 6082 alloy DC-casting billet with a diameter of 380 mm. The experiment result shows that after the pulsed magnetic field melt treatment, the morphology of α-Al grains in the billet changed from coarse dendritic to small globular and its size was reduced by 18.5–45.4% compared to the existing process. Meanwhile, the difference in morphology of α-Al between the billet centre and edge decreased at the same time. This work may provide a new method for the grain refinement of the 6082 alloy DC-casting billet.

Keywords: 6082 alloy; grain refinement; pulsed magnetic field melt treatment; DC-casting; microstructural analysis

Citation: Bao, X.; Ma, Y.; Liu, Y. Microstructure Evolution in a 6082 Alloy under Pulsed Magnetic Field Melt Treatment. *Eng. Proc.* **2023**, *43*, 30. https://doi.org/10.3390/engproc2023043030

Academic Editor: Mario Fafard

Published: 19 September 2023

1. Introduction

The 6xxx series aluminium alloys contain magnesium and silicon as the main additional elements. They are widely used in the manufacturing of trusses, bridges, automotive components and structural profiles of aircraft structures, which are produced by forging or rolling [1–3]. The most commonly used raw material for the forging or rolling process is the direct-chilling (DC)-casting billet. However, the significant improvement in mechanical properties results from grain refinement of the DC-casting billet [4]. Therefore, it is necessary to control the solidification structure of the DC-casting billet. At present, the most common method of refining the solidification structure is to add master alloys such as Al-Ti-B, Chromium (Cr) element or Al-Ti-C into the melt during the DC-casting process [5–7]. In recent years, with the development of the physical field, the ultrasonic field [8,9] and electromagnetic field [10] have been applied in the DC-casting process for solidification structure refinement. Due to the advantage of not having contact with the melt, the application of an electromagnetic field in DC-casting has attracted more attention than other grain refining methods.

Inspired by the previous work [11,12], the pulsed magnetic field was applied in the 6082 alloy DC-casting process to refine the solidified structure of the 380 mm diameter billet. In this work, the pulsed magnetic field generator was located on the top of the launder as shown in Figure 1, unlike the conventional pulsed magnetic field casting, which is a coil located around the crystallizer [10]. Meanwhile, grain refinement comparison research between the pulsed magnetic field treatment (PMMT) and Al-5Ti-1B grain refiner was

conducted. The results of this work may provide a new method to refine the solidification structure of the 6082 alloy DC-casting billet.

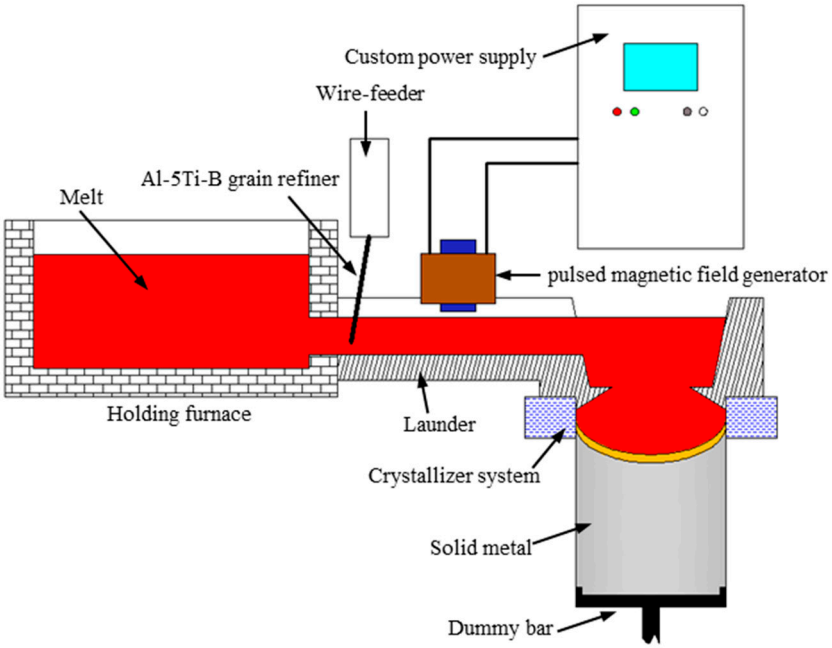

Figure 1. Schematic diagram of the device used in this study.

2. Experimental Details

The experimental device used in the present study is shown in Figure 1. The device consists of three parts, including a launder and crystallizer system of DC-casting, a set of pulsed magnetic field generators located on the top of the launder and a custom power supply. In the beginning, the raw materials for the 6082 alloy were melted in the melting furnace. The composition of the alloy was analyzed by a direct-reading spectrometer and is given in Table 1. Then, the melt was transformed into the holding furnace and prepared for casting. During the casting, the melt flowed to the crystallizer through the launder from the holding furnace. The diameter of the as-cast billet was 380 mm. The casting temperature was 705 °C. The casting speed was 60 mm/min. Meanwhile, the cooling water flow rate was 23 m^3/h and the temperature was 25 °C.

Table 1. Chemical composition of the 6082 alloy used in the experiment.

Elements	Si	Fe	Cu	Mn	Mg	Cr	Zn	Al
wt.%	1.0	0.5	0.1	0.7	1.0	0.25	0.2	Bal.

Four conditions were applied in the casting process. At the beginning of the casting, the melt was cast without the Al-5Ti-1B grain refiner and not treated by the pulsed magnetic field. While the billet length was 500 mm, the custom power supply was initiated, and the pulsed magnetic field generator loaded the current with the peak value 200 A, frequency 20 Hz and duty cycle 20%. The melt was treated by the pulsed magnetic field while it flowed through the pulsed magnetic field generator. When the casting length was 1100 mm, the Al-5Ti-1B grain refiner wire was added to the melt, and the addition of the Al-5Ti-1B grain refiner was 0.27 wt.%. While the casting length was 1700 mm, the custom power supply was turned off. The grain refiner was added until the billet length was 2300 mm. The whole casting process was continuous. Finally, the testing samples were taken from casting billets and did not receive any additional heat treatment.

Several sheets having a thickness of about 20 mm were cut from the billet along the cross-section under different casting conditions. The specimens utilized for the microstructure observation were cut from the centre, 1/2 R and edge of the sheet, as shown in Figure 2. All samples were carefully polished and etched with a Keller's solution (5 mL HNO_3, 3 mL HCl and 2 mL HF in 190 mL distilled water) for 1 min. Then, the microstructure was observed by an optical microscope (Axio Observer Z1, Carl Zeiss). For quantitative analysis, the size of the α-Al was measured through the linear intercept method according to the Chinese standard GB 6394-2017, and the result is an average of five photos. The hardness tests of the samples were carried out at room temperature. The Vickers hardness (HV) in the centre and $\frac{1}{2}$ R were measured by the Vickers hardness tester (Q10A+, Qness), and the result for each sample is the average of 10 testing points.

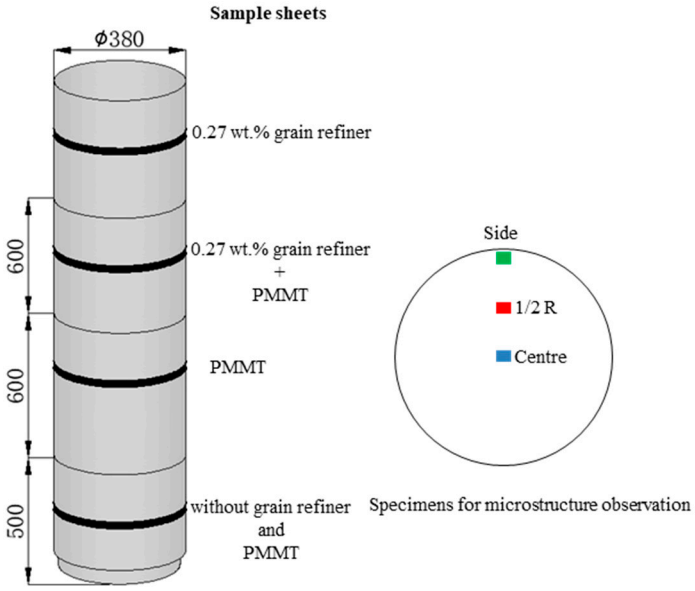

Figure 2. Schematic illustration of samples for microstructure observation.

3. Result and Discussion

3.1. Solidification Structure

The microstructure of the 6082 alloy DC-casing billet under different casting conditions is shown in Figure 3. In the condition without the grain refiner and PMMT, the morphology of α-Al grains is mainly coarse dendrites in the billet centre and course equiaxed grains in the billet edge, as shown in Figure 3a,c, respectively. When the PMMT was applied, there were smaller equiaxed grains that appeared both on the billet centre and 1/2R, while there was no significant change in the billet edge, as shown in Figure 3d,e,f, respectively. When the 0.27 wt.% grain refiner was added into the melt and combined with the PMMT, the morphology of α-Al grains was fine equiaxed crystal grains in the billet cross-section, as shown in Figure 3g,h,i, respectively. When the PMMT was terminated, the morphology of α-Al grains was still equiaxed grains, but their size had a relatively significant increase compared to the previous condition, as shown in Figure 3j–l.

The size of α-Al grains is given in Figure 4. As compared to the condition without the grain refiner and PMMT, the α-Al size in the billet centre decreased from 178.78 μm to 137.25 μm, while the 1/2 R of the billet decreased from 179.53 μm to 146.40 μm. When the 0.27 wt.% grain refiner was added, the α-Al size in the billet centre was 138.64 μm and 133.7 μm in the 1/2 R. It can be concluded that the PMMT has almost the same grain refinement effect as the grain refiner. When the 0.27 wt.% grain refiner was combined with the PMMT, it could achieve the smallest α-Al grains size, which is 116.10 μm, 111.40 μm and 88.26 μm in the billet centre, 1/2 R and edge, respectively.

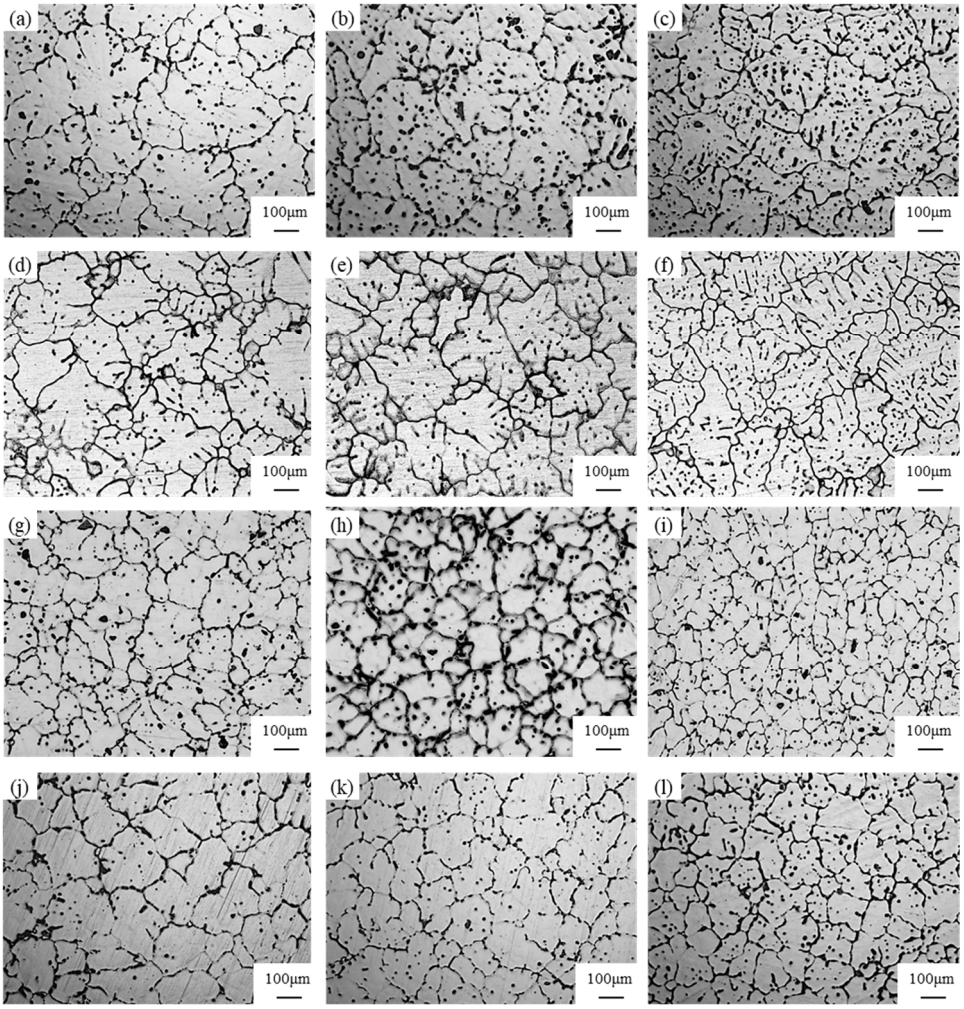

Figure 3. The microstructure of the billet under different casting conditions: without grain refiner and PMMT: (**a**) centre, (**b**) 1/2 R, (**c**) edge; the PMMT: (**d**) centre, (**e**) 1/2 R, (**f**) edge; 0.27 wt.% grain refiner combined with PMMT: (**g**) centre, (**h**) 1/2 R, (**i**) edge; 0.27 wt.% grain refiner: (**j**) centre, (**k**) 1/2 R, (**l**) edge.

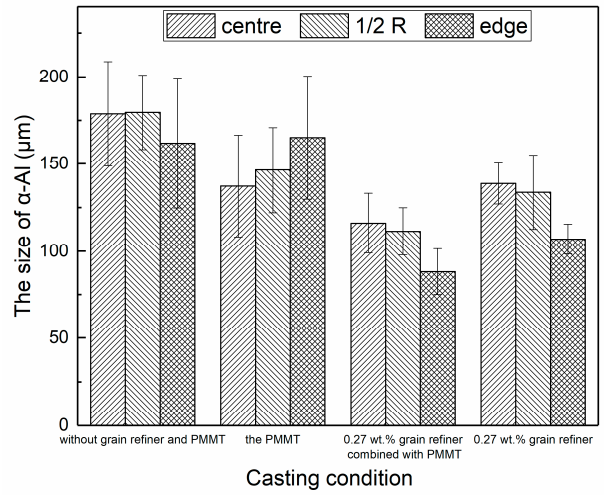

Figure 4. The size of α-Al grains under different casting conditions.

It is well known that the increase of the nucleation rate is the main reason for the solidification structure being refined. When the melt was treated by the pulsed magnetic

field, the energy of the pulsed magnetic field permeated into the melt, leading to the number of the larger clusters being increased in the melt [13]. During the solidification, larger clusters transformed into nuclei in a short time, leading to an increase in the nucleation rate [14]. Meanwhile, those larger clusters are distributed on the whole melt, thus the nuclei will appear on the whole cross-section of the billet during the solidification, leading to the solidification structure being refined in the billet centre compared to the condition without the grain refiner and PMMT. When the PMMT was combined with the 0.27 wt.% grain refiner, a heterogeneous nucleation factor such as $TiAl_3$ and TiB_2 was released due to the grain refiner melting, leading to the further increase of the nuclei, thus the finest solidification structure formed under this condition.

3.2. Hardness Measurement

As mentioned before, the solidification structure was refined after the pulsed magnetic field melt treatment. Figure 5 is the Vickers hardness under different casting conditions. As shown in Figure 5, in the condition without the grain refiner and the PMMT, the Vickers hardness is 62.7 Hv in the centre and 68.3 Hv in the 1/2 R. When the PMMT was applied, the Vickers hardness increased to 65.4 Hv in the centre and 70.9 Hv in the 1/2 R. Under the condition of the 0.27 wt.% grain refiner, the Vickers hardness is 67.4 Hv in the centre and 70.1 Hv in the 1/2 R. It can be seen that the improvement of the Vickers hardness under the condition of the PMMT is nearly the same as the addition of the grain refiner. When the PMMT was combined with the 0.27 wt.% grain refiner, the Vickers hardness reached 76.6 Hv and 88.7 Hv in the centre and 1/2 R, respectively. Due to the grains becoming considerably finer, the Vickers hardness at room temperature is improved due to the effect of fine-grain strengthening [15].

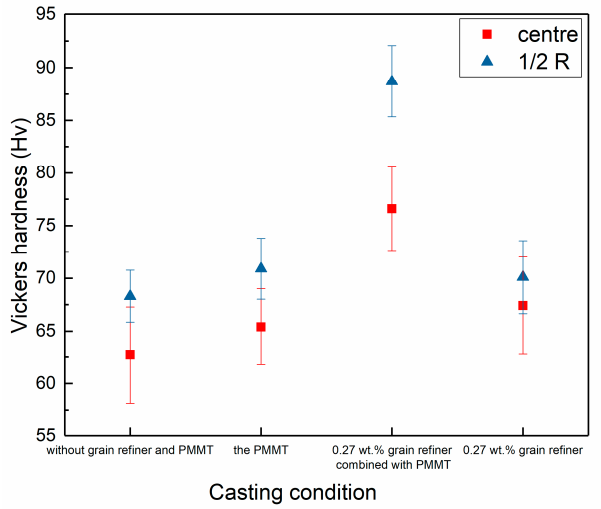

Figure 5. The Vickers hardness in different casting conditions.

4. Conclusions

The pulsed magnetic field melt treatment (PMMT) was successfully applied on the commercial 6082 alloy DC-casting billet with a diameter of 380 mm to manipulate the microstructure. The main conclusions are as follows.

(1) The solidification structure of the 6082 alloy DC-casting billet with a diameter of 380 mm can be refined through the pulsed magnetic field melt treatment.

(2) The Vickers hardness has increased in the billet centre and 1/2 R after the pulsed magnetic field melt treatment due to the effect of fine-grain strengthening.

(3) The grain refinement of the pulsed magnetic field melt treatment is nearly the same as the grain refiner. While the finest solidification structure can be achieved with a combination of both.

Author Contributions: Conceptualization, Y.M. and X.B.; methodology, Y.M. and X.B.; validation, Y.M.; formal analysis, X.B., Y.L. and Y.M.; investigation, X.B. and Y.L.; resources, Y.M.; data curation, X.B. and Y.L.; writing—original draft preparation, X.B.; writing—review and editing, X.B. and Y.M.; supervision, Y.M.; project administration, Y.M. and Y.L. All authors have read and agreed to the published version of the manuscript.

Funding: This research received no external funding.

Institutional Review Board Statement: Not applicable.

Informed Consent Statement: Not applicable.

Data Availability Statement: Not applicable.

Conflicts of Interest: The authors declare no conflict of interest.

References

1. Kumar, N.; Goel, S.; Jayaganthan, R.; Owolabi, G.M. The influence of metallurgical factors on low cycle fatigue behavior of ultra-fine grained 6082 Al alloy. *Int. J. Fatigue* **2018**, *110*, 130–143. [CrossRef]
2. Kumar, N.; Goel, S.; Jayaganthan, R.; Brokmeier, H.G. Effect of grain boundary misorientaton, deformation temperature and AlFeMnSi-phase on fatigue life of 6082 Al alloy. *Mater. Charact.* **2017**, *124*, 229–240. [CrossRef]
3. Foydl, A.; Segatori, A.; Khalifa, N.B.; Donati, L.; Brosius, A.; Tomesani, L.; Tekkaya, A.E. Grain size evolution simulation in aluminium alloys AA 6082 and AA 7020 during hot forward extrusion process. *Mater. Sci. Technol.* **2013**, *29*, 100–110. [CrossRef]
4. Widlicki, P.; Garbacz, H.; Lewandowska, M.; Pachla, W.; Kulczyk, M.; Kurzydlowski, K.J. The Influence of Hydrostatic Extrusion on the Microstructure of 6082 Aluminium Alloy. *Solid State Phenom.* **2006**, *114*, 145–150. [CrossRef]
5. Izcankurtaran, D.; Tunca, B.; Karatay, G. Investigation of the Effect of Grain Refinement on the Mechanical Properties of 6082 Aluminium Alloy. *Open J. Appl. Sci.* **2021**, *11*, 699–706. [CrossRef]
6. Schempp, P.; Cross, C.E.; Schwenk, C.; Rethmeier, M. Influence Of Ti And B Additions On Grain Size And Weldability Of Aluminium Alloy 6082. *Weld. World* **2013**, *56*, 95–104. [CrossRef]
7. Quested, T.E. Understanding mechanisms of grain refinement of aluminium alloys by inoculation. *Mater. Sci. Technol.* **2004**, *20*, 1357–1369. [CrossRef]
8. Yin, Z.; Le, Q.; Chen, X.; Jia, Y. The grain refinement of Mg alloy subjected to dual-frequency ultrasonic melt treatment: A physical and numerical simulation. *J. Mater. Res. Technol.* **2022**, *21*, 1554–1569. [CrossRef]
9. Koli, Y.; Yuvaraj, N.; Aravindan, S.; Vipin. Enhancement of Mechanical Properties of 6061/6082 Dissimilar Aluminium Alloys Through Ultrasonic-Assisted Cold Metal Transfer Welding. *Arab. J. Sci. Eng.* **2021**, *46*, 12089–12104. [CrossRef]
10. Li, H.; Liu, S.; Jie, J.; Guo, L.; Chen, H.; Li, T. Effect of pulsed magnetic field on the grain refinement and mechanical properties of 6063 aluminum alloy by direct chill casting. *Int. J. Adv. Manuf. Technol.* **2017**, *93*, 3033–3042. [CrossRef]
11. Bai, Q.; Ma, Y.; Xing, S.; Bao, X.; Feng, Y.; Yu, W.; Kang, X. Effect of flow, heat transfer and magnetic energy on the grain refinement of 7A04 alloy under electromagnetic pulse. *Int. J. Mater. Res.* **2017**, *108*, 1064–1072. [CrossRef]
12. Bai, Q.; Ma, Y.; Xing, S.; Bao, X.; Feng, Y.; Kang, X. Nucleation and grain refinement of 7A04 aluminum alloy under a low-power electromagnetic pulse. *J. Mater. Eng. Perform.* **2018**, *27*, 857–863. [CrossRef]
13. Bao, X.; Ma, Y.; Xing, S.; Liu, Y.; Shi, W. Effects of Pulsed Magnetic Field Melt Treatment on Grain Refinement of Al-Si-Mg-Cu-Ni Alloy Direct-Chill Casting Billet. *Metals* **2022**, *12*, 1080–1094. [CrossRef]
14. Vekilov, P.G. The two-step mechanism of nucleation of crystals in solution. *Nanoscale* **2010**, *2*, 2346–2357. [CrossRef] [PubMed]
15. Tian, L.; Guo, Y.; Li, J.; Xia, F.; Liang, M.; Bai, Y. Effects of solidification cooling rate on the microstructure and mechanical properties of a cast Al-Si-Cu-Mg-Ni piston alloy. *Materials* **2018**, *11*, 1230. [CrossRef] [PubMed]